Volume 60
Number 47
14 June 2024
Pages 5991–6072

ChemComm

Chemical Communications

rsc.li/chemcomm

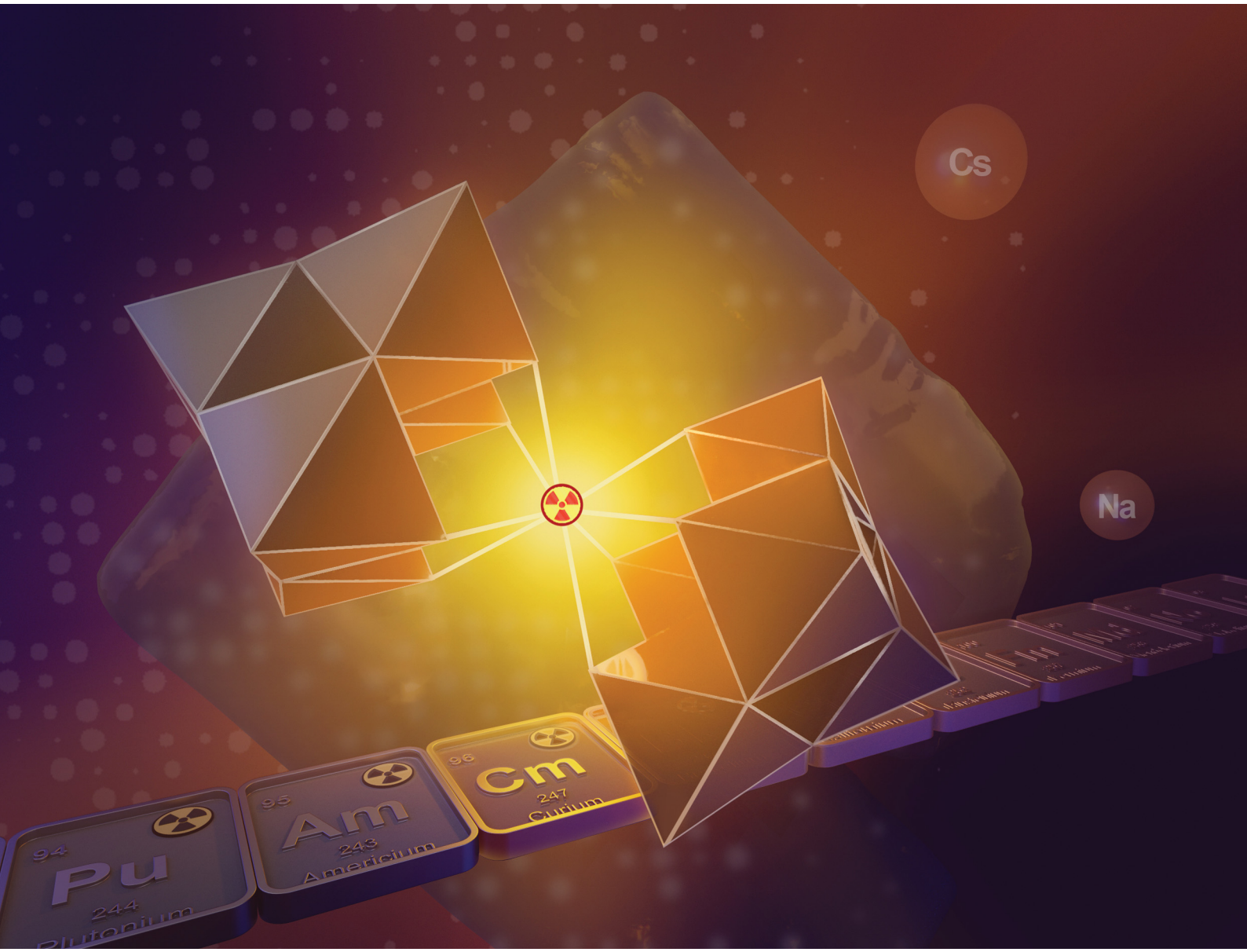

ISSN 1359-7345

ROYAL SOCIETY OF CHEMISTRY

COMMUNICATION

Ian Colliard and Gauthier J.-P. Deblonde
Characterization of the first Peacock–Weakley polyoxometalate containing a transplutonium element: curium bis-pentatungstate $[Cm(W_5O_{18})_2]^{9-}$

60 YEARS ANNIVERSARY

ChemComm

COMMUNICATION

View Article Online
View Journal | View Issue

Cite this: *Chem. Commun.*, 2024, **60**, 5999

Received 26th March 2024,
Accepted 8th May 2024

DOI: 10.1039/d4cc01381f

rsc.li/chemcomm

Characterization of the first Peacock–Weakley polyoxometalate containing a transplutonium element: curium bis-pentatungstate $[Cm(W_5O_{18})_2]^{9-}$†

Ian Colliard*[ab] and Gauthier J.-P. Deblonde*[ac]

Leveraging microgram-level techniques, we here present the first transplutonium bis-pentatungstate complex: $NaCs_8Cm(W_5O_{18})_2 \cdot 14H_2O$ (CmW_5). Single crystal XRD, Raman, and fluorescence characterization show significant differences relative to analogous lanthanide compounds. The study reveals the unsuspected impact of counterions on fluorescence and vibrational modes of the curium complex and its lanthanide counterparts.

Interests in polyoxometalates can be traced as far back as the 19th century, with the synthesis of ammonium phosphomolybdate $(NH_4)_3(PMo_{12}O_{40})$ first reported in 1826.[1] Since then, polyoxometalates, POMs, have permeated into various other fields, ranging from drug delivery to microelectronics, catalysts, energy storage, and more.[2–6] POMs can also act as metal chelators and, while their chemistry is incredibly diverse, POMs are typically derived from a handful of major structures, with notably, the Peacock–Weakley[7] *e.g.*, $[M^{n+}(W_5O_{18})_2]^{15-n}$, the Lindqvist[8] (*e.g.*, $Nb_6O_{19}^{8-}$), the Keggin[9] (*e.g.*, $PMo_{12}O_{40}^{n-}$), the Well–Dawson[10] (*e.g.*, $P_2W_{18}O_{62}^{6-}$), the Preyssler[11] (*e.g.*, $[M^{n+}P_5W_{30}O_{110}]^{15-n}$) ions, *etc.*

Perhaps not surprisingly, compared to other fields, POM chemistry has had little overlap with actinide chemistry thus far, and particularly for heavy actinides (Am, Cm, Bk, Cf…). The first instance of a polyoxometalate compound containing an actinide was reported in 1914, with the synthesis of a thorium(IV) polymolybdate $(NH_4)_8(ThMo_{12}O_{42})$.[12] However, it is not until after the 1970's that a renewed interest in incorporating actinide elements into polyoxometalate chemistry yielded additional structures. Moreover, while the actinide group consists of fifteen members, most of the data published on actinide POMs is about thorium and uranium. The high specific activity and isotope scarcity are only some of the constraints that have limited studies with transuranic elements. Recently, certain POMs have been leveraged to crystallize their complexes in microgram quantities,[13,14] opening the avenue to studying their interactions with elements beyond plutonium (Fig. 1a). However, the number of known actinide POMs with transplutonium elements is still very limited: only one with Am(IV),[15] one with americyl(VI),[16] and three with Cm(III).[13]

One class of POMs that has historically received strong interest is the bis-pentatungstate–metal complex $[M^x(W_5O_{18})_2]^{(12+x)-}$. Intense luminescent and optical properties when complexing lanthanide (Ln) ions, in solution and solid-state,[17–20] provide strong motivation to pursue analogous compounds with transplutonium ions, notably Cm^{3+}, as it can undergo fluorescence with a wide variety of ligands.[21–23] Unlike the other POM structures that can complex metal ions, such as the Keggin or the Well–Dawson anions, the pentatungstate anion $[W_5O_{18}]^{6-}$ (W_5), is often considered as the smallest and simplest POM ligand, both in terms of structure and synthesis. Fluorescence studies on aqueous solutions of W_5 and Cm^{3+} previously showed[13] a ~500 times increase in the luminescence of Cm^{3+} upon complexation to W_5,

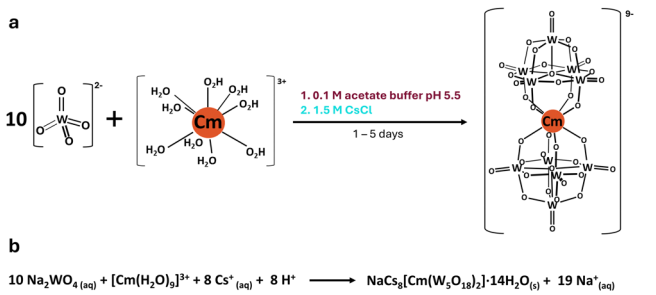

Fig. 1 Reaction scheme (a) and equation (b) for forming the curium bis-pentatungstate complex $[Cm(W_5O_{18})_2]^{9-}$. The starting curium(III) aqua ion is considered to have 9 water molecules, as previously reported by Skanthakumar *et al.*[24]

[a] *Physical and Life Sciences Directorate, Glenn T. Seaborg Institute, Lawrence Livermore National Laboratory, Livermore, California 94550, USA. E-mail: Colliard1@LLNL.gov, Deblonde1@LLNL.gov*
[b] *Material Sciences Division, Lawrence Livermore National Laboratory, Livermore, California 94550, USA*
[c] *Nuclear and Chemical Sciences Division, Lawrence Livermore National Laboratory, Livermore, California 94550, USA*

† Electronic supplementary information (ESI) available. CCDC 2333195 and 2326544. For ESI and crystallographic data in CIF or other electronic format see DOI: https://doi.org/10.1039/d4cc01381f

with a shift and splitting of the emission peaks (598.4 to 604.6 nm with multiple Stark levels). By analogy to the lanthanides, the expected complex formed in solution was $[Cm(W_5O_{18})_2]^{9-}$ (CmW_5). CmW_5 solutions exhibit the longest fluorescence lifetime for a Cm^{3+} complex reported so far (780 μs), and we hypothesized[13] it was due to the complete removal of water molecules from the starting $[Cm(H_2O)_9]^{3+}$ aqua ion (Fig. 1b).[24] However, the crystal structure of this kind of heavy actinide complex has remained elusive.

Herein we report the single crystal XRD structure of CmW_5, which represents the first heavy actinide compound of the Peacock–Weakley POM class. The cesium salt of CmW_5, fully formulated as $NaCs_8[Cm(W_5O_{18})_2]\cdot 14H_2O$, crystallizes in the anorthic space group $P\bar{1}$ (V = 2711.36 (6) Å^3). We further report the first $[Ln(W_5O_{18})_2]^{9-}$ compound with cesium counterions, $Na_3Cs_6[Nd(W_5O_{18})_2]\cdot 18H_2O$, which crystallizes in the anorthic space group $P\bar{1}$ (V = 2811.36 (6) Å^3). While the only distinguishable feature between the heavy actinide and the lanthanide is a difference in the number of Na^+ and Cs^+ counterions, the apparent crystallographic divergence preludes the spectroscopic differences observed for these compounds both in solution and solid-state, as discussed below.

A prior attempt to isolate this compound as a rubidium or cesium salt failed,[13] but a cesium salt of CmW_5 was here successfully isolated as single crystals (Fig. 3) by modifying our recently developed microgram-level POM–metal complex synthesis.[13] In this optimized synthesis, we only used 1.2 μg of $^{247/246/248}Cm^{3+}$, starting from a HCl solution (see Experimental section in the ESI†). Note that XRD-quality single crystals of CmW_5 could only be grown with Cs^+ counterions (Fig. 3c and d). Yet, the structure is isomorphic with previously reported sodium and potassium salts of $[Ln^{III}(W_5O_{18})_2]^{9-}$ (Table S1, ESI†) and $[An^{IV}(W_5O_{18})_2]^{8-}$ (An = Th, U, and Np).[17,25] Briefly, the structure is comprised of two $[W_5O_{18}]^{6-}$ ligands coordinating a central Cm^{3+}. The W_5 ligand is built upon five edge-sharing octahedral tungstates, four of which corner-share to the central Cm^{3+} ion, forming an eight-coordinate square antiprismatic coordination environment for curium, with a nearly ideal D_{4d} symmetry. Bond lengths range 2.459(9)–2.508(9) Å for Cm–O, 1.715(6)–1.740(10) Å for W–$O^{terminal}$, 2.348–1.776 Å for W–$O^{bridging}$, and 2.967(10)–3.762(10) Å for Cs–$O^{Cm's}$. See ESI† for additional information on the synthesis and structure of CmW_5.

Interestingly, no water molecule is present in the first coordination sphere of the Cm^{3+} ion, which contrasts with previously studied heavy actinide complexes with organic ligands which are typically 9-coordinated and often have actinide-bound water molecules.[24,26,27] Moreover, in all the other W_5 reported structures with trivalent lanthanides (Table S1, ESI†), the Na^+ counterions bind to several water molecules instead of direct ion-pairing with the POM observed for the Cs–CmW_5 structure. The lanthanide structures mainly featured hydrogen bonding interactions between the $[Ln^{III}(W_5O_{18})_2]^{9-}$ and the $[Na(H_2O)_n]^+$ counterions. On the other hand, the CmW_5 salt reported herein is the only instance thus far of the W_5 complex crystallizing with Cs counterions.

The most noticeable effect of the Cs counterions is the complete removal of the 9 water molecules from the Cm^{3+} aqua ion,[24] and it manifests as increased bonding interactions among Cs^+ ions, the POM, and the central actinide ion. Of the eight Cs counterions in the CmW_5 structure, five are close to curium (Cs–Cm distance of 4.48–4.54 Å) and bind directly to the bridging O in Cm–O–W (Cs–O^{Cm} distance of 2.967(10)–3.762(10) Å). The lone Na^+ counterion found in the structure at ~7 Å from Cm^{3+} favors binding with solvated water molecules, similar to what is observed in the lanthanide structures, and it only binds with the tungstate POMs *via* one yl oxygen between two complexes (Fig. 2). The interplay among Cm^{3+}, W_5, and Cs^+ ion leads to a unique geometry where Cm^{3+} is completely shielded from solvent molecules and surrounded by eight oxygens at ~2.48 Å, and five Cs^+ at ~4.51 Å (Fig. 2).

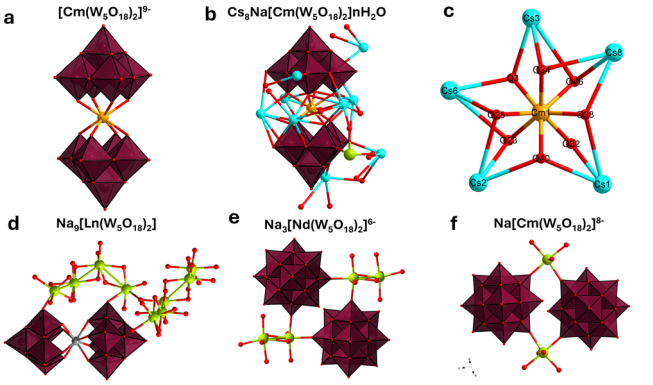

Fig. 2 Polyhedral representations of the CmW_5 and NdW_5 compounds. (a) The $[Cm(W_5O_{18})_2]^{9-}$ complex, with counterions and solvated water molecules for clarity. (b) Asymmetric unit of the Cs–CmW_5 crystal, fully formulated as $NaCs_8[Cm(W_5O_{18})_2]\cdot 14H_2O$. (c) Closeup view of the $[CmO_8]$ square antiprismatic coordination, with five Cs counterions binding to all eight oxygens. (d) Asymmetric unit of the Na_9NdW_5 structure,[13] showing no connectivity between complexes, (e) connectivity between complexes for $Na_3Cs_6[Nd(W_5O_{18})_2]$. (f) Connectivity between complexes for $NaCs_8[Cm(W_5O_{18})_2]\cdot nH_2O$. Color code: Cm (orange), Cs (light blue), Na (green), W (maroon octahedra), O (red).

Control experiments were performed with Nd^{3+} (Fig. 2 and 3), as its size[28] is similar to Cm^{3+}, by synthesizing both a cesium salt (Cs–NdW_5) and a sodium salt (Na–NdW_5). For Cm, a solid sample was also prepared with Na^+ counterions (Na–CsW_5) but only micro to sub-microcrystals could be obtained (Fig. 3d) so that no single crystal XRD characterization could be performed. Raman microscopy experiments on $Na_9[Ln^{III}(W_5O_{18})_2]$ previously assigned the characteristics bands[13,17]: 980–920 cm^{-1} for the terminal yl'O stretching (W═O), 850–500 cm^{-1} for the bridging O stretching in W–O–W, <350 cm^{-1} for various vibrational modes for the entire complex, and lastly peaks at 890 and 200 cm^{-1} correspond to the bridging O stretching in Ln–O–W. The Raman spectrum of Na–NdW_5 is consistent with previously reported spectra.[13,17] Interestingly, we observed a clear effect of the Cs^+ counterions (Fig. 3b) with combined changes in Raman peak intensities and peak shifting. Although Raman intensities can typically vary slightly from crystal to crystal, significant differences were observed between CmW_5 and NdW_5. For CmW_5, the intensities of the terminal yl oxygens (W═O) increase, which could be due to increased Cs-complex interactions. For Nd–O–W, there is a decrease in intensity for the 890 cm^{-1} peak and an increase for the 211 cm^{-1} peak, which

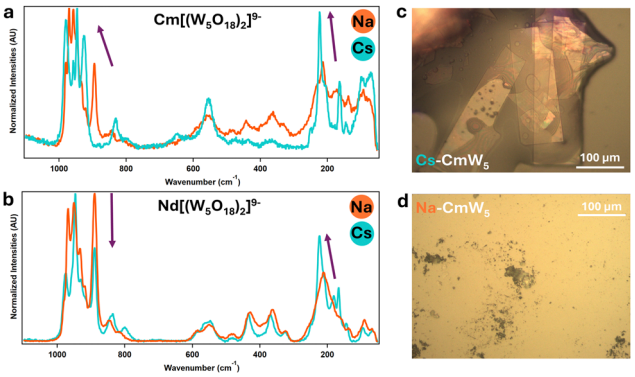

Fig. 3 Solid-state Raman microscopy of CmW_5 and $Nd–W_5$ (a) $[Cm(W_5O_{18})_2]^{9-}$ with sodium (in orange) and cesium (in blue) counterions. (b) Similar experiments with $[Nd(W_5O_{18})_2]^{9}$. (c) CCDC image capture of $Cs–CmW_5$ single crystals. This picture was taken under UV-light – the pink-orange fluorescence highlights the presence of Cm^{3+}. (d) $Na–CmW_5$ solution evaporated onto a microscopy slide. The material was crystalline, but the crystals were too small for XRD analysis. See Fig. S1 (ESI†) for additional crystal pictures.

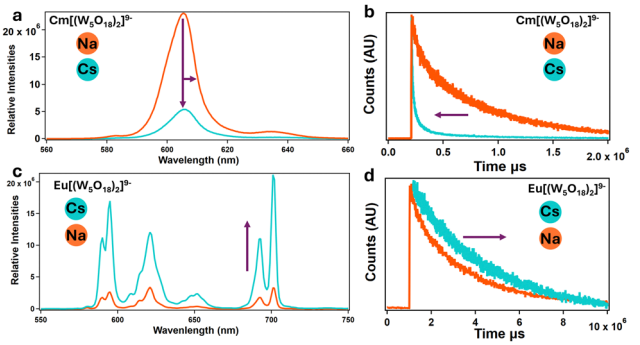

Fig. 5 Solution and time-resolved fluorescence. (a) and (b) Emission spectra of solutions of CmW_5 with sodium and cesium counterions, showing fluorescence quenching and lifetime shortening. (c) and (d) Similar experiments with NdW_5, showing opposite behavior. Both CmW_5 and EuW_5 complexes are under 100 mM acetate buffer at a pH of 5.5. $[EuW_5]$ = 1 mM. $[CmW_5]$ = 100 µM ($Cs–CmW_5$ spectra was adjusted to compensate for the dilution for the addition of 3 M CsCl, final concentration of $Cs–CmW_5$ was 50 µM). See Fig. S4 and S5 (ESI†) for corresponding excitation spectra.

also shifts to 223 cm^{-1}. For CmW_5, an increase in Raman intensity for the terminal O and bridging O and peak shifting from 211 to 223 cm^{-1} is also observed (Fig. 3a). However, the 890 cm^{-1} peak corresponding to Cm–O–W is shifted to higher energy by 35 cm^{-1} to 925 cm^{-1}, *i.e.*, the opposite of what is observed for the $Na/Cs–NdW_5$ compounds. The blue shifting caused by the Cs on the bridging O in Cm–O–W is a clear indicator of the outsized role Cs^+ ions on the $[Cm(W_5O_{18})_2]^{9-}$ complex as opposed to its lanthanide analogs. To the best of our knowledge, this represents the first observation of cesium–actinide interactions within a molecular complex.

The impact of Cs counter ions on CmW_5 was further investigated *via* fluorescence spectroscopy (Fig. 4 and 5). We recently

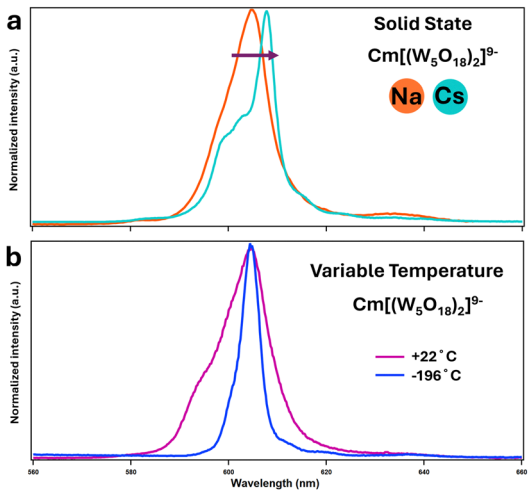

Fig. 4 (a) Solid-state emission spectra of $[Cm(W_5O_{18})_2]^{9-}$ with Na and Cs counterions (b) fluorescence emission of aqueous solutions of $Na–CmW_5$ at room temperature (22 °C – pink curve) and after flash-freezing in liquid nitrogen (−196 °C – blue curve). Solvent: 1 : 4 vol/vol glycerol : H_2O. Excitation wavelength: 271.0 nm. See Fig. S2 and S3 (ESI†) for corresponding excitation spectra.

reported[13] solution-state fluorescence experiments on $Na–CmW_5$. The Cm^{3+} emission peak is centered at 604.6 nm and the fluorescence lifetime decay of 780 µs is the longest observed for a Cm^{3+} complex in solution. We performed similar Cm^{3+} fluorescence experiments with and without cesium counterions, and both in the solid-state (Fig. 4) and solution-state (Fig. 5). Consistent with the Raman spectroscopy results, the fluorescence properties of CmW_5 were also found to be impacted by the nature of the counterions. Fig. 4a shows the emission spectrum of single crystals of $Cs–CmW_5$ and a crystalline precipitate of $Na–CmW_5$. Switching the counterions from Na to Cs, the Cm^{3+} emission peak shifts from 604.6 to 608.0 nm. The structure of the emission peak of $Cs–CmW_5$ is also more pronounced, likely indicative of less disorder in the structure. We also measured the emission spectrum of $Na–CmW_5$ in solution at room temperature and as a flash-frozen solution at liquid-nitrogen temperature (−196 °C). The spectrum of the $Na–CmW_5$ solution (Fig. 4b) at room temperature is consistent with that of the solid (Fig. 4a). Upon cooling, the $Na–CmW_5$ emission peak becomes more structured, and we could confirm the main emission band is at 604.6 nm, consistent with the solid-state data. The results clearly indicate that the nature of the counterion impacts the energy levels of CmW_5.

To further confirm the results, Fig. 4a shows the emission spectra of a $Na–CmW_5$ solution (consistent with previously reported data[13]) and the same sample after addition of Cs^+ counterions. A significant quenching of the luminescence is observed, with the emission intensity decreasing by an order of magnitude. A shortening of the lifetime to about 515 µs and a peak shifting from 604.6 to 606.0 nm were also observed (Fig. 5a and b). This strongly indicates that Cs^+ counterions, typically considered spectator ions, actually influence bonding and energy levels within the CmW_5 complex.

The relatively close proximity between Cm^{3+} and Cs^+ ions in the crystal structure (Fig. 2) suggests that Cs^+ may provide a relaxation pathway for Cm^{3+} upon excitation, akin to water

molecules, hence leading to shortening of the luminescence lifetime. Another hypothesis is that ion-pairing formation between Cs and W_5 is strong enough to change the excited state energy levels of the POM, leading to less efficient fluorescence sensitization of Cm^{3+} luminescence.

Similar solution-state experiments were performed with Eu^{3+}, due to its relatively similar size to Cm^{3+} and fluorescence properties (Fig. 5c and d). Solutions of Na–EuW_5 exhibit the typical multi-peak emission band of a Eu^{3+} complex, with main peaks at ~680, ~620, ~650, and ~700 nm (Fig. 5c). The measured fluorescence lifetime of 2385 μs indicates that no water molecule is present.[29] However, contrary to curium, when an excess of Cs^+ ions is added, the emission intensity of EuW_5 increases significantly, by a factor of ~10, and the lifetime increases from 2385 to 3431 μs. This, combined with the Cm results indicate the Cs ions impact the energy levels of the POM.

In conclusion, this study reports the first example of a Weakley–Peacock-type polyoxometalate complex with a transplutonium element, namely the curium bis-pentatungstate $NaCs_8Cm(W_5O_{18})_2 \cdot 14H_2O$. This compound was synthesized at the microscale and characterized *via* single crystal XRD, Raman microscopy, as well as solid-state and solution-state fluorescence. Comparative experiments with Nd^{3+} and Eu^{3+} analogous compounds revealed a divergence between lanthanide and actinide coordination chemistries. This study further highlights the unsuspected but critical impact that counterions, particularly cesium, have on the fluorescence and vibrational modes of $[Cm(W_5O_{18})_2]^{9-}$. These results show that, even within the same coordination chemistry framework (*i.e.*, 8-coordinated complexes with square antiprismatic geometry), 4f and 5f cations exhibit fundamental chemical differences that can be manifested at long-range and even *via* interactions with other cations present in the structure. Given the high number of heavy tungsten atoms in the POM compounds, in addition to many oxygens and presence of the heavy actinide, computational work (*e.g.*, density functional theory) to explain the fundamental origin of these experimental observations are currently too expensive. Further compounding this, the results presented herein indicate that computational treatment of f-element POM complexes will require considering the full lattice (not just $[Cm(W_5O_{18})_2]^{9-}$, for example), including all cesium or sodium counterions and water molecules. Future work will focus on expanding the experimental space for actinide–POM compounds in order to provide a consistent framework for future theoretical work on this, so far, overlooked class of actinide compounds.

This material is based upon work supported by the U. S. Department of Energy, Office of Science, Office of Basic Energy Sciences, Heavy Element Chemistry program at Lawrence Livermore National Laboratory under Contract DE-AC52-07NA27344. Release number: LLNL-JRNL-861963.

Conflicts of interest

There are no conflicts to declare.

Notes and references

1 M. T. Pope and A. Müller, *Angew. Chem., Int. Ed. Engl.*, 1991, **30**, 34–48.
2 C. Busche, L. Vilà-Nadal, J. Yan, H. N. Miras, D.-L. Long, V. P. Georgiev, A. Asenov, R. H. Pedersen, N. Gadegaard, M. M. Mirza, D. J. Paul, J. M. Poblet and L. Cronin, *Nature*, 2014, **515**, 545–549.
3 J.-J. Chen, M. D. Symes and L. Cronin, *Nat. Chem.*, 2018, **10**, 1042–1047.
4 A. Gaita-Ariño, F. Luis, S. Hill and E. Coronado, *Nat. Chem.*, 2019, **11**, 301–309.
5 N. Gao, H. Sun, K. Dong, J. Ren, T. Duan, C. Xu and X. Qu, *Nat. Commun.*, 2014, **5**, 3422.
6 D. Wang, L. Liu, J. Jiang, L. Chen and J. Zhao, *Nanoscale*, 2020, **12**, 5705–5718.
7 R. D. Peacock and T. J. R. Weakley, *J. Chem. Soc. A*, 1971, 1836–1839.
8 I. Lindqvist, *Ark. Kemi*, 1953, **5**, 247–250.
9 J. F. Keggin and W. L. Bragg, *Proc. R. Soc. London, Ser. A*, 1997, **144**, 75–100.
10 B. Dawson, *Acta Crystallogr.*, 1953, **6**, 113–126.
11 M. T. Pope, *Heteropoly and Isopoly Oxometalates*, Springer, Berlin, Heidelberg, 1983.
12 M. T. Pope, in *Structural Chemistry of Inorganic Actinide Compounds*, ed.S. V. Krivovichev, P. C. Burns and I. G. Tananaev, Elsevier, Amsterdam, 2007, pp. 341–361.
13 I. Colliard, J. R. I. Lee, C. A. Colla, H. E. Mason, A. M. Sawvel, M. Zavarin, M. Nyman and G. J.-P. Deblonde, *Nat. Chem.*, 2022, **14**, 1357–1366.
14 C. A. Colla, I. Colliard, A. M. Sawvel, M. Nyman, H. E. Mason and G. J.-P. Deblonde, *Inorg. Chem.*, 2023, **62**, 6242–6254.
15 M. N. Sokolova, A. M. Fedosseev, G. B. Andreev, N. A. Budantseva, A. B. Yusov and P. Moisy, *Inorg. Chem.*, 2009, **48**, 9185–9190.
16 H. Zhang, A. Li, K. Li, Z. Wang, X. Xu, Y. Wang, M. V. Sheridan, H.-S. Hu, C. Xu, E. V. Alekseev, Z. Zhang, P. Yan, K. Cao, Z. Chai, T. E. Albrecht-Schönzart and S. Wang, *Nature*, 2023, **616**, 482–487.
17 W. P. Griffith, N. Morley-Smith, H. I. S. Nogueira, A. G. F. Shoair, M. Suriaatmaja, A. J. P. White and D. J. Williams, *J. Organomet. Chem.*, 2000, **607**, 146–155.
18 K. Zheng and P. Ma, *Dalton Trans.*, 2024, **53**, 3949–3958.
19 M. Shiddiq, D. Komijani, Y. Duan, A. Gaita-Ariño, E. Coronado and S. Hill, *Nature*, 2016, **531**, 348–351.
20 H. Zhang, X. Li, L. Zhang, Y. Zhou, X. Ren and M. Liu, *J. Alloys Compd.*, 2018, **749**, 229–235.
21 C. Adam, B. B. Beele, A. Geist, U. Müllich, P. Kaden and P. J. Panak, *Chem. Sci.*, 2015, **6**, 1548–1561.
22 S. K. Cary, J. Su, S. S. Galley, T. E. Albrecht-Schmitt, E. R. Batista, M. G. Ferrier, S. A. Kozimor, V. Mocko, B. L. Scott, C. E. Van Alstine, F. D. White and P. Yang, *Dalton Trans.*, 2018, **47**, 14452–14461.
23 G. J.-P. Deblonde, J. A. Mattocks, H. Wang, E. M. Gale, A. B. Kersting, M. Zavarin and J. A. Cotruvo, *J. Am. Chem. Soc.*, 2021, **143**, 15769–15783.
24 S. Skanthakumar, M. R. Antonio, R. E. Wilson and L. Soderholm, *Inorg. Chem.*, 2007, **46**, 3485–3491.
25 P. Villars, K. Cenzual, R. Gladyshevskii, O. Shcherban, V. Dubenskyy, V. Kuprysyuk, I. Savysyuk and R. Zaremba, in *Structure Types. Part 11: Space groups (135) P42/mbc – (123) P4/mmm*, ed. P. Villars and K. Cenzual, Springer Berlin Heidelberg, Berlin, Heidelberg, 2012, vol. 43A11, pp. 213–214.
26 M. J. Polinski, D. J. Grant, S. Wang, E. V. Alekseev, J. N. Cross, E. M. Villa, W. Depmeier, L. Gagliardi and T. E. Albrecht-Schmitt, *J. Am. Chem. Soc.*, 2012, **134**, 10682–10692.
27 S. S. Galley, S. A. Pattenaude, C. A. Gaggioli, Y. Qiao, J. M. Sperling, M. Zeller, S. Pakhira, J. L. Mendoza-Cortes, E. J. Schelter, T. E. Albrecht-Schmitt, L. Gagliardi and S. C. Bart, *J. Am. Chem. Soc.*, 2019, **141**, 2356–2366.
28 R. D. Shannon, *Acta Crystallogr.*, 1976, **A32**, 751–767.
29 J. Bruno, W. D. Horrocks and R. J. Zauhar, *Biochemistry*, 1992, **31**, 7016–7026.

